**CST-1032**

# Impact of Geometric Uncertainties on Pump Performance

Pansaporn Sribonfha[1], Sirod Sirisup[1,*] and Vejapong Juttijudata[2]

[1] National Electronics and Computer Technology Center, Pathumthani, Thailand 12120
[2] Department of Aerospace Engineering, Faculty of Engineering, Kasetsart University, Bangkok, Thailand 10900
* Corresponding Author: sirod.sirisup@nectec.or.th, Tel: +662-564-6900 ext 2275 Fax: +66 25646776

***Abstract***

A reverse engineer of an existing design of a pump is a common practice of small local pump manufacturers. With in-house low-cost manufacturing processes, the final dimension and geometry of the pump can be deviated from those in the original pump design. These geometric uncertainties due to manufacturing variability usually lead to serious implications on the performance of the pump. The goal of this study is to analyze the impact of geometric uncertainties of the pump on its performance. Different parameters characterizing geometric uncertainties are considered. The variation of head and efficiency of the pump due to geometric uncertainties are then examined for different flow rates at a given rotational speed by means of CFD simulation. To this end, the method of moments is employed to propagate these uncertainties through CFD simulation process. Only mean and variance of pump head and efficiency with respect to statistically independent, random and normally distributed input geometric uncertainties are accounted for in the current study. Here, the first-order sensitivity derivatives needed in the moment methods are derived through adjoint model. The effects of each input geometric uncertainty to pump performance variation will be fully discussed. Critical geometric parameters will be identified from the first-order sensitivity derivatives. The result can be used as a guideline for geometric tolerancing in manufacturing processes.

***Keywords**: geometric uncertainties pump performance, uncertainty analysis, moment methods, adjoint model.*

## 1. Introduction

In-house low-cost manufacturing processes of small local pump manufacturers could result in a serious geometric deviation from the geometry of the nominal design from reverse engineering processes of existing pumps. Similar studies on geometric variability of compressor geometries [1-3] suggest it could have profound effect in the performance of compressor and a robust design could improve the performance under geometric variability.

Due to a small number of geometric parameters in those studies, direct methods were used to determine the sensitivity of these parameters and surrogate models were developed. Adjoint method commonly used in shape optimization e.g. [4] and can be used to quantify uncertainties in model parameters in computational models [5-6] is an alternative method when number of geometric parameters is large.

The objective of this study is to analyze the impact of geometric uncertainties of the pump on its performance by means of adjoint approach and the method of moments. Assumption in this study is the geometric variability is rather small and thus the moment methods can be used to provide linear approximation of the performance deviation. The result can be a useful guideline geometric tolerancing in manufacturing processes and robust design for manufacturability.

## 2. Theory

### 2.1 Computational Fluid Dynamics (CFD)

In this study we use the Reynolds-Averaged Navier-Stokes (RANS) equations. The RANS equations are well documented for example see [7]. We rather provide brief details here. In brief, the RANS equations can be written as follows:

$$\frac{\partial \bar{\mathrm{U}}}{\partial \mathrm{t}} + \mathrm{div}(\bar{\mathrm{U}}\mathbf{U}) = -\frac{1}{\rho}\frac{\partial \mathrm{P}}{\partial \mathrm{x}} + \upsilon \mathrm{div}\big(\mathrm{grad}(\bar{\mathrm{U}})\big) + \frac{1}{\rho}\left[\frac{\partial\left(-\rho\overline{\mathrm{u}'^2}\right)}{\partial \mathrm{x}} + \frac{\partial(-\rho\overline{\mathrm{u}'\mathrm{v}'})}{\partial \mathrm{y}} + \frac{\partial(-\rho\overline{\mathrm{u}'\mathrm{w}'})}{\partial \mathrm{z}}\right]$$

$$\frac{\partial \bar{\mathrm{V}}}{\partial \mathrm{t}} + \mathrm{div}(\bar{\mathrm{V}}\mathbf{U}) = -\frac{1}{\rho}\frac{\partial \mathrm{P}}{\partial \mathrm{y}} + \upsilon \mathrm{div}\big(\mathrm{grad}(\bar{\mathrm{V}})\big) + \frac{1}{\rho}\left[\frac{\partial(-\rho\overline{\mathrm{u}'\mathrm{v}'})}{\partial \mathrm{x}} + \frac{\partial\left(-\rho\overline{\mathrm{v}'^2}\right)}{\partial \mathrm{y}} + \frac{\partial(-\rho\overline{\mathrm{v}'\mathrm{w}'})}{\partial \mathrm{z}}\right]$$

$$\frac{\partial \bar{\mathrm{W}}}{\partial \mathrm{t}} + \mathrm{div}(\bar{\mathrm{W}}\mathbf{U}) = -\frac{1}{\rho}\frac{\partial \mathrm{P}}{\partial \mathrm{z}} + \upsilon \mathrm{div}\big(\mathrm{grad}(\bar{\mathrm{W}})\big) + \frac{1}{\rho}\left[\frac{\partial(-\rho\overline{\mathrm{u}'\mathrm{w}'})}{\partial \mathrm{x}} + \frac{\partial(-\rho\overline{\mathrm{v}'\mathrm{w}'})}{\partial \mathrm{y}} + \frac{\partial\left(-\rho\overline{\mathrm{w}'^2}\right)}{\partial \mathrm{z}}\right]$$

Here, the Reynolds stresses terms are modeled by the RNG k-$\varepsilon$ model.

### 2.2 The method of moments

The primary interest of the current study is to calculate the deviation bounds e.g. the mean and standard deviation of an objective function, e.g. pump performance, after some geometric uncertainties have been included to the nominal design. To this end, we have chosen the method of moments to propagate such uncertainties through the simulation process [8-9]. For a given objective function $J$, the method of moments is based on the Taylor's series expansion of the objective function about the mean of input $\bar{\boldsymbol{q}}$ and the associated standard deviation $\sigma_{q_i}$. The resulting mean and variance of the objective function with first order approximation are as follows:

$$\bar{J} = J(\bar{\boldsymbol{q}}) \tag{1}$$

$$Var_J = \sum_{i=1}^{N}\left(\left.\frac{dJ}{dq_i}\right|_{\bar{\boldsymbol{q}}} \sigma_{q_i}\right)^2 \tag{2}$$

Where $\left.\frac{\partial J}{\partial q_i}\right|_{\bar{\boldsymbol{q}}}$ is the gradient of $J$ or the sensitivities of the objective function $J$ with respect to input $\boldsymbol{q}$. One can also derive the higher order approximations as well but these approximations will involve the higher derivatives of the objective function $J$ with respect to input $\boldsymbol{q}$.

### 2.3 Objective function gradient

It is obvious that in order to utilize method of moments to propagate uncertainty, the objective function sensitivity or gradient is needed. If the number of input is small, the sensitivity can be easily computed by finite differences or other similar direct approaches. However, it is not the case when dimension of the input space grows. To efficiently derive the sensitivity, we follow the adjoint approach. Here, we provide overall description of the approach. First, we can explicitly rewrite our objective function $J$, as $J = J(\boldsymbol{q}) = J(\boldsymbol{q}, \boldsymbol{X})$ where $\boldsymbol{X}$ is the state variables satisfy the nonlinear state equation $\psi(\boldsymbol{q}, \boldsymbol{X}) = 0$ e.g the RANS equations. Thus for each $q_i$ component in $\boldsymbol{q}$,

$$\frac{dJ}{dq_i} = \frac{\partial J}{\partial q_i} + \frac{\partial J}{\partial \boldsymbol{X}}\frac{d\boldsymbol{X}}{dq_i} \tag{3}$$

The differentiation of the state equation with respect to input is now read:

$$\frac{\partial \psi}{\partial q_i} + \frac{\partial \psi}{\partial \boldsymbol{X}}\frac{d\boldsymbol{X}}{dq_i} = 0 \tag{4}$$

This equation allows us to compute the state sensitivities, $\theta_i = \frac{d\boldsymbol{X}}{dq_i}$, by solving linear system defined as:

$$\frac{\partial \psi}{\partial \boldsymbol{X}}\theta_i = -\frac{\partial \psi}{\partial q_i} \tag{5}$$

Thus in order to get the objective function sensitivities e.g. Eq 3, we first compute Eq. 5 and substitute the state sensitivities in Eq. 3. However, we need to solve the linear system, Eq. 5 for each input component $q_i$, resulting in inefficiency approach for if the dimension of the input becomes large. The adjoint approach proposes that we can combine Eqs. 3-4 in the transposed form as:

$$\left(\frac{dJ}{d\boldsymbol{q}}\right)^T = \left(\frac{\partial J}{\partial \boldsymbol{q}}\right)^T - \left(\frac{\partial \psi}{\partial \boldsymbol{q}}\right)^T \left(\left(\frac{\partial \psi}{\partial \boldsymbol{X}}\right)^T\right)^{-1} \left(\frac{\partial J}{\partial \boldsymbol{X}}\right)^T \tag{6}$$

then we can compute the gradient by first solving the adjoint system

$$\left(\frac{\partial \psi}{\partial \boldsymbol{X}}\right)^T \chi = \left(\frac{\partial J}{\partial \boldsymbol{X}}\right)^T \tag{7}$$

Where $\chi$ is the adjoint variable and then by computing

$$\left(\frac{dJ}{d\boldsymbol{q}}\right)^T = \left(\frac{\partial J}{\partial \boldsymbol{q}}\right)^T - \left(\frac{\partial \psi}{\partial \boldsymbol{q}}\right)^T \chi \tag{8}$$

Using the adjoint approach, we need to solve only one linear system for any number of the input space dimension. In this study, we use the ANSYS Fluent adjoint solver to calculate the objective function gradient. Precisely, we can extract the objective function gradient through the shape sensitivity variables in the ANSYS Fluent adjoint solver [10]. The details of the extraction is presented in section 4.

## 3. Methodology

### 3.1 Nominal pump design

Our simulation model was constructed by considering the submersible pump that consists of ten backward curved blades presented in Figure 1. Profiles of each blade are designed by the arc-tangent method which aims to smooth the flow streamline travelled along the blade. This pump was created according to the characteristic variables and dimension shown in table 1 [11-12].

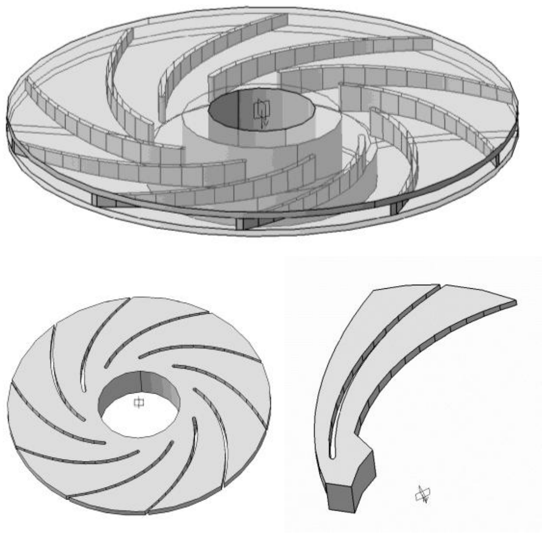

Fig. 1 Nominal pump geometry

Table. 1 The geometry of the nominal pump design

| Geometric Variables | |
|---|---|
| $D_1/D_2$ | 3.2300 cm/7.600 cm |
| Blade inlet angle ($\beta_1$) | 33.1656° |
| Blade outlet angle ($\beta_2$) | 40° |
| Inlet passage width ($b_1$) | 0.4257 cm |
| Outlet passage width ($b_2$) | 0.1874 cm |
| Rotating speed | 2850 rpm |
| Inlet pressure | 2560 Pa |
| Outlet pressure | 10000-45000 Pa |

The boundary conditions are set based on the characteristics in Table 1 as well.

The head and efficiency have been numerically estimated based on simulation approach through the computational fluid dynamics (CFD) with Reynolds-averaged Navier-Stokes (RANS) equations where the RNG k-$\varepsilon$ model equation with standard wall function has been used as the turbulence model. All simulations have been performed using the ANSYS Fluent software.

Since the impeller is axial symmetric, the flow behavior of each blade section could assume to be identical. Therefore, we just need to perform on the one-tenth of the impeller fluid domain with axial symmetric assumption. The submersible impeller fluid domain contains 103,036 nodes and 539,823 elements, respectively, see Figure 1. Fluid domain is modeled as incompressible flow with rotating frame motion. The casing wall and impeller blade are set as moving walls.

The simulation of the nominal model has been conduct in two stages. The first stage is to evaluate the nominal design performance for various flow rates. Here, we vary the outlet pressure on a specific number; 10000 Pa, 30000 Pa and 45000 Pa respectively to estimate head as well as efficiency. The second stage is to perform the adjoint calculation using the ANSYS Fluent adjoint solver. The adjoint solver needs the previously computed direct solver solution. Here we have provided one of the three cases from the previous stage. Specifically, we have provided the solution from the 10000 Pa case, as demonstration case. Besides, due to the limitation of the ANSYS Fluent adjoint solver, for our study, we need to provide the corresponding velocity inlet profile to the ANSYS Fluent adjoint solver as well. We need to specify the objective function for the adjoint solver to compute for its sensitivities. Here, we provide the total pressure rise between inlet and outlet boundaries as our objective function. Overall, we have observed that the computational time required to run the ANSYS Fluent adjoint solver is about 20% more than that needed to run the direct solver. As the ANSYS Fluent adjoint solver converges, the solver provides the shape sensitivities that are required for uncertainty propagation with the method of moments.

## 4. Results

### 4.1 Nominal design performance

The head and efficiency of the nominal design for various scenarios are shown in table 2.

Figure 3-4 shows the increased pressure at outlet. In Figure 5, we also present the overall flow path lines along the impeller.

Table. 2 Nominal design's head and efficiency

| Outlet Pressure | Head (m) | Efficiency (%) |
|---|---|---|
| 10000 Pa | 2.0230 | 45.82 |
| 30000 Pa | 3.5164 | 60.53 |
| 45000 Pa | 4.6695 | 61.51 |

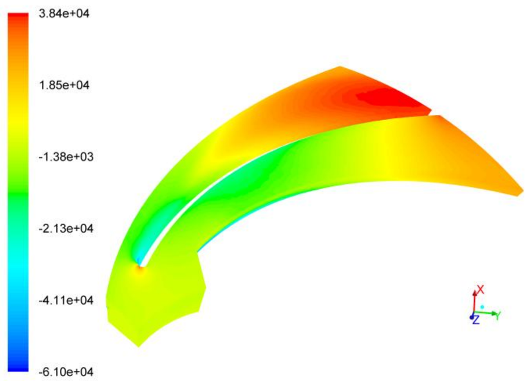


Fig. 2 Total pressure distribution (Pa)

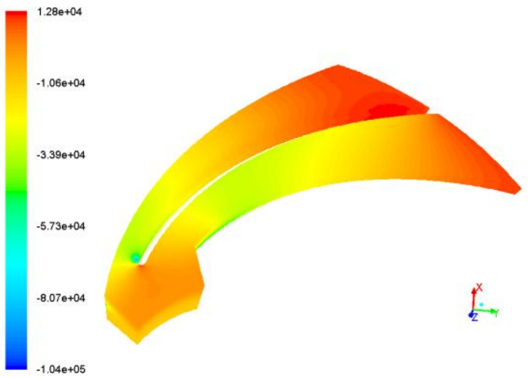


Fig. 3 Static pressure distribution (Pa)

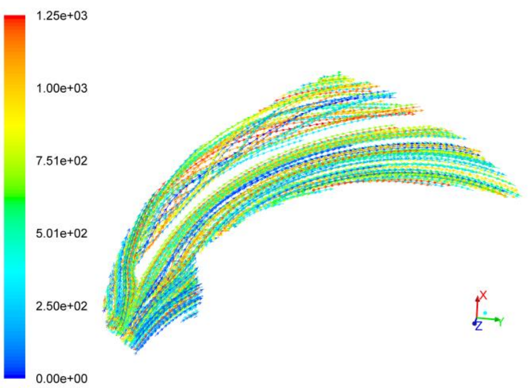


Fig. 4 Flow path lines

**4.2 Uncertainty propagation**

We need to calculate the mean and the variance of our objective function, the total pressure rise, after the impeller blade geometric uncertainties have been introduced. Here, we chose to propagate the impeller blade geometric uncertainties through the method of moments. From section 2, we know that the method requires the objective function gradient to compute the variance of the objective function under given uncertainty. However, the objective function gradient is not directly available from the ANSYS Fluent adjoint solver but rather only its pattern is available from shape sensitivities variables, shown in Figure 5. The extremely large shape sensitivities magnitudes are also found in other studies [13].

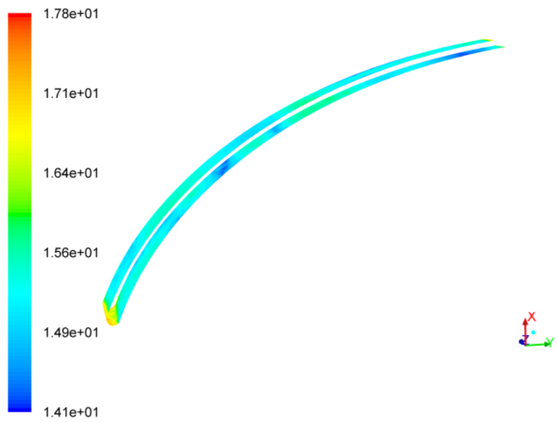


Fig. 5 Shape sensitivity magnitude in log scale.

In order to find the objective function gradient from the shape sensitivities, we need to find a scaling factor, $\lambda$. This scaling factor can be found from another ANSYS Fluent direct solver calculation with only slight modification on the impeller blade geometry.

From total differential of $J$:

$$dJ = \frac{\partial J}{\partial x}dx + \frac{\partial J}{\partial y}dy + \frac{\partial J}{\partial z}dz$$
$$= \lambda\left(\frac{\widehat{\partial J}}{\partial x}dx + \frac{\widehat{\partial J}}{\partial y}dy + \frac{\widehat{\partial J}}{\partial z}dz\right) \quad (9)$$

where $\frac{\widehat{\partial J}}{\partial x}, \frac{\widehat{\partial J}}{\partial y}, \frac{\widehat{\partial J}}{\partial z}$ are shape sensitivities obtained from the ANSYS Fluent adjoint solver. Thus, once total differential of $J$ is known from the new ANSYS Fluent direct solver run, we can obtain the scaling factor $\lambda$ and finally the actual objective function gradient.

Specifically, in the current investigation, we first run the ANSYS Fluent direct solver with our nominal design to obtained the total pressure rise between the inlet and outlet boundaries. We then perform the ANSYS Fluent adjoint solver run in order to obtain the shape sensitivities of the objective function. Then we run the ANSYS Fluent direct solver again but now with the slight modification of the impeller blade to obtain the objective function differential. Finally we employ Eq. 9 to obtain the objective function gradient.

From the objective function gradient, as well as the shape sensitivities, shown in Figure 5, it emphasizes the fact that the total pressure rise strongly depends on the location of the impeller blade leading edge. Besides, the trailing edge of suction side also shows high sensitivities as well. Once the cost function gradient has been found, we can now investigate the propagation of the impeller blade geometric uncertainties through the method of moments. Here, we assume that the mean input is the nominal blade design itself. Precisely, the input variables represent the locations of the blade profile. Table 3 summarizes the propagation of the uncertainties in various ways and in major section of the blade.

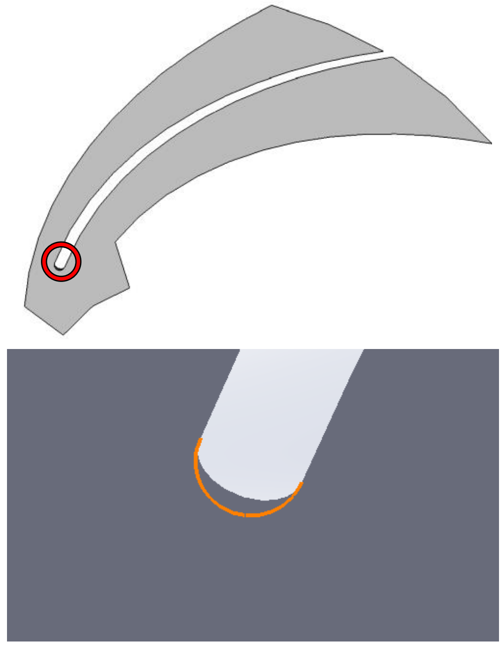

Fig. 6 Modification of impeller blade geometry: Orange line indicates the outline of the nominal design.

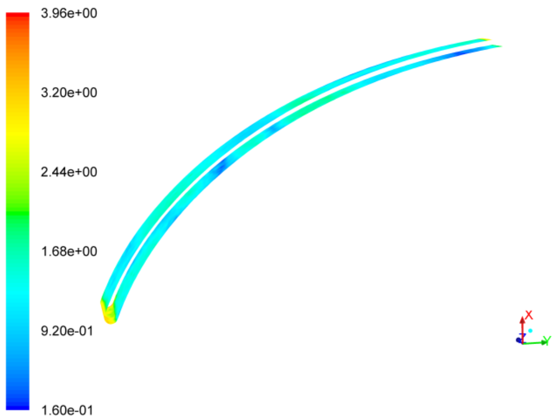


Fig. 7 Magnitude of the objective function gradient in log scale.

In calculation for the uncertainty propagation in Table 3, we also assume that the standard deviations in each location are the in the same order for each dimension e.g. the standard deviation in the first column written in terms of *(p,q,r)* represents individual location standard deviation of *p, q* and *r* in *x, y* and *z* directions, respectively.

Table. 3 Variance of total pressure rise given blade displacement uncertainties

| Input standard deviation | Variance of total pressure rise ($Pa^2$) | |
|---|---|---|
| | Whole | Leading edge |
| (1mm, 1mm, 1mm) | 4488.833 | 4163.223 |
| (1mm, 0, 0) | 1810.963 | 1711.281 |
| (0, 1mm, 0) | 2175.848 | 1982.783 |
| (0, 0, 1mm) | 502.022 | 469.159 |
| (1mm, 1mm, 0) | 3986.811 | 3694.064 |
| (1mm, 0, 1mm) | 2312.985 | 2180.440 |
| (0, 1mm, 1mm) | 2677.870 | 2451.942 |
| (1cm, 1cm, 1cm) | 398681.2 | 369406.5 |

From table 3, the results suggest that the total pressure rise deviations mostly result from the blade impeller displacements in both *x* and *y* directions. The uncertainties in *z* direction contribute only 10% of the total variance. The results also show that the major deviation is contributed mainly (about 90%) from the leading edge displacements. This conforms to the gradient magnitude in Figure 7. This kind of information is valuable in providing guideline for geometric tolerancing in impeller blade manufacturing processes. Finally, we also see that deviation results do show the linear behavior of the first order approximation by the method of moments.

## 5. Conclusion

The aim of this paper is to investigate uncertainty propagation with the method of moments. The demonstration case chosen here is the investigation in impact of impeller blade geometric uncertainties on centrifugal pump's performance. The total pressure rise is chosen to be the main target in assessing the performance. In order to employ the method of moments to propagate the uncertainties, we need the objective cost function gradient. The ANSYS Fluent adjoint solver has been used to provide the gradient derived through its shape sensitivity output. The results from the uncertainties propagation suggests that the major impact are from the blade geometric uncertainties in the blade leading edge as well as *x* and *y* directions. These results can be used as a guideline for geometric tolerancing in centrifugal pump manufacturing processes.

## 6. Acknowledgements

The authors acknowledge the WATA cluster of Kasetsart University for providing computing resources.

## 7. References

[1] Javed, A., Pecnik, R., Olivero, M. and van Buijtenen, J.P., Effects of Manufacturing Noise on Microturbine Centrifugal Impeller Performance, ASME Journal of Engineering for Gas Turbines and Power, Vol. 134, Issue 10 (2012), pp. 102-302.

[2] Garzon, V.E. and Darmofal, D.L., Impact of Geometric Variability on Axial Compressor Performance, ASME Journal of Turbomachinery, Vol. 125, No. 4, (2003), pp. 692–703.

[3] Kumar, A, Keane, A.J, Nair, R.B. and Shahpar, S., Robust Design of Compressor Fan Blades Against Erosion, ASME Journal of

Mechanical Design, Vol. 128(4), (2006), pp. 864-873.

[4] Jameson, A. and Ou, K., Optimization Methods in Computational Fluid Dynamics, Encyclopedia of Aerospace Engineering, Edited by Richard Blockley and Wei Shyy, John Wiley & Sons, 2010.

[5] Fidkowski, K.J., Darmofal, D.L., Review of output-based error estimation and mesh adaptation in computational fluid dynamics, (2011), AIAA Journal, 49 (4), pp. 673-694.

[6] Sherman, L. L., Taylor III, A. C., Green, L. L., and Newman, P. A., First- and second-order aerodynamic sensitivity derivatives via automatic differentiation with incremental iterative methods, Journal of Computational Physics , Vol. 129, 1996, pp. 307-331.

[7] Versteeg, H. K., Malalasekera, W., An Introduction to Computational Fluid Dynamics. The Finite Volume Method (2007), second edition.

[8] Putko, M. M., Newmann, P. A., Taylor III, A. C., and Green, L. L., Approach for uncertainty propagation and robust design in CFD using sensitivity derivatives," AIAA Paper, 2001-2528, June 2001.

[9] Putko, M. M., Newman, P. A., Taylor III, A.C. Employing sensitivity derivatives to estimate uncertainty propagation in CFD. In: 9th ASCE Specialty Conference on Probabilistic Mechanics and Structural Reliability. 2004, pp. 1-6.

[10] ANSYS. Fluent Adjoint Solver User's Guide. Fluent Inc.; 2011.

[11] Charoenkijtavee, T., Juttijudata, V. and Arundachawat, P. (2006). Performance Analysis for Submersible Pump -A Numerical Approach, paper presented in *the Annual National Symposium on Computational Science & Engineering 2006*, Chiang Mai, Thailand.

[12] Techanaoharak, K. and Viriyasavettakul, T., Design to Improve the Imperller of Industrail Pump, *Aerospace Engineering Senior Project Report 2005 [in Thai]*, Kasetsart University.

[13] Zaya, J., Aerodynamic Optimization of Ground Vehicles with the Use of Fluent’s Adjoint Solver, Master’s Thesis, Department of Applied Mechanics, Chalmers University of Technology, 2013.